Fabrication of hydroxyapatite sponges by dextran sulphate/amino acid templating

Rosanna Gonzalez-McQuire[a,*], David Green[b], Dominic Walsh[a], Simon Hall[a], Jean-Yves Chane-Ching[c], Richard O.C. Oreffo[b], Stephen Mann[a]

[a]*Centre for Organized Matter Chemistry, School of Chemistry, University of Bristol, Bristol BS8 1TS, UK*
[b]*Bone & Joint Research Group, University of Southampton, Southampton SO16 6YD, UK*
[c]*Rhodia Recherches, 52 Rue de la Haie Coq, Aubervilliers 93308, Cedex, France*

Abstract

We report a new template-directed method for the fabrication of hydroxyapatite (HAp) sponges by using amino-acid-coated HAp nanoparticles dispersed within a viscous polysaccharide (dextran sulfate) matrix, and describe the use of these materials for the viability and proliferation of human bone marrow stromal cells. The nanoparticles were prepared in the presence of excess amounts of aspartic acid, alanine or arginine, and subsequently organised into macroporous frameworks with typical pore sizes of 100–200 μm during thermal degradation of the dextran matrix. The sponge macrostructure was influenced by changes in the heating rate and sintering time, as well as the use of different amino acids or variations in dextran functional groups. Biocompatibility testing showed retention of cell viability, production of extracellular matrix and alkaline phosphatase expression, suggesting that it should be possible to exploit this novel fabrication method for potential applications in cartilage or soft tissue engineering.

1. Introduction

Hydroxyapatite (HAp)-based scaffolds for potential use in tissue engineering have been recently prepared using a range of novel methods involving foaming [1,2] or dissolvable [3] polymers, biomacromolecular/HAp composites [4,5], or electrophoretic deposition of preformed particles [6]. One drawback to these methods is the general difficulty in tailoring materials properties whilst maintaining the pre-requisites of scaffold design [7], such as large pore sizes (100–400 μm) [8], non-toxicity, biocompatibility [9], osteoconductivity [10] and osteoinductivity [11].

In this paper, we report a new method for the fabrication of HAp sponges by using amino-acid-coated HAp nanoparticles dispersed within a viscous polysaccharide (dextran sulfate) matrix, and describe the use of these materials for the viability and proliferation of human bone marrow stromal cells. The nanoparticles are prepared in the presence of excess amounts of aspartic acid, alanine or arginine [12], and subsequently organized into macroporous frameworks during thermal degradation of a dextran gel under controlled heating. This approach, which was used recently to prepare metallic and metal oxide sponges [13], involves the in situ aggregation and coalescence of nanoparticles into interconnecting rods or filaments specifically at the gas–solid interface of CO_2 and O_2 gas bubbles formed during pyrolitic decomposition of the dextran paste. Although dextran, which is a polysaccharide consisting of D-glucose with α-1,6-linkages, is known to interact with various metallic and ceramic surfaces [14–17], the use of interactions between the polysaccharide matrix and other organics to regulate the assembly of preformed nanoparticles has not to our knowledge been previously demonstrated.

Corresponding author.
E-mail address: r.gonzalez-mcquire@bris.ac.uk (R. Gonzalez-McQuire).

2. Materials and methods

2.1. HAp nanoparticles and sponges

In brief, amino acid-functionalised HAp nanoparticles were prepared by hydrothermal treatment of calcium phosphate-containing solutions in the presence of aspartic acid, alanine or arginine at pH 9. The solutions were prepared by room temperature addition of aqueous Na_2HPO_4 to an aqueous solution containing $CaCl_2$ and amino acid at a Ca^{2+}:-PO_4^{3-}:amino acid molar ratio of 3:1:6. Typically 11.10 g of $CaCl_2$ and an appropriate amount of the amino acid (26.6 g for aspartic acid) were dissolved in 100 mL of distilled water followed by the addition of NaOH (5 M) to adjust the pH to 9. The final [Ca^{2+}] was 1 M. Aqueous Na_2HPO_4 (0.33 mM) was prepared by dissolving 11.94 g of $Na_2HPO_4 \cdot 12H_2O$ in 100 mL distilled water. This was then added dropwise to the calcium/amino acid mixture whilst adjusting the pH to 9 with NaOH. The reaction mixture was aged in a round-bottom flask whilst stirring for 16 h at 60 °C, after which a colloidal dispersion of nanorods was obtained for samples prepared in the presence of arginine and alanine. Alternatively, a white precipitate was formed by slow aggregation in the presence of aspartic acid.

HAp sponges were prepared as follows. Dextran sulfate powder ($M_w = 500$k) was dissolved in the HAp/amino acid suspension, containing 2.8 wt% of HAp nanoparticles, in a 3:2 (w/w) ratio; typically 15 g dextran sulfate was added to 10 mL of the HAp dispersion. The mixture was manually stirred to produce a viscous paste that was transferred to a petri dish and left to air dry for 7 days. The resulting materials were then heated at a rate of 10°/min to 800 °C and left at this temperature for 6 h. Samples for SEM (JEOL JSM 5600 LV) were mounted on aluminium stubs with carbon tape and coated in Pt. UV–vis spectroscopy was carried out on solid samples before heating using a Perkin Elmer Lambda 25 spectrometer. XRD (Philips PW 1800 diffractometer, CuKα radiation) and FT-IR spectroscopy (Perkin-Elmer spectrum one) were performed on crushed materials. Similar experiments were undertaken using unfunctionalised dextran ($M_w = 500$k) as sacrificial template.

2.2. Cell studies

Primary cultures of human bone marrow (HBM) stromal cells were harvested using minimal essential medium—alpha modification (αMEM) from trabecular bone marrow samples obtained from patients undergoing routine total hip replacement surgery. (Only tissue that would have been discarded was used with the approval of the Southampton General Hospital Ethics Committee). The cells were pelleted at 4 °C by centrifugation at 500*g* for 5 min, resuspended in 10 mL αMEM, and passaged through nylon mesh (90 μm pore size; Lockertex, Warrington, England). Samples of the cell suspension were diluted with 0.5% (w/v) trypan blue in 0.16 M ammonium chloride and the number and viability of nucleated cells were determined. Cultures were fed every 5 days and maintained at 37 °C and 5%CO_2 in basal media (αMEM supplemented with 10% FCS) for up to 3 weeks unless otherwise stated. All studies were conducted using human cells after one passage. Following trypsinisation and re-suspension in FCS-free αMEM, 2×10^5 HBM stromal cells were seeded onto sterilised fragments of UV-irradiated HAp/D or HAp/A sponges, or grown in αMEM supplemented with 10% FCS as a positive control.

HBM stromal cells were incubated with Cell Tracker™ green (5-chloromethylfluorescein diacetate, CFMDA) (Molecular Probes, Leiden, Netherlands) and Ethidium Homodimer-1 (EH-I) (Molecular Probes, Leiden, Netherlands) for 45 min to label viable and necrotic cells, respectively. The media were then replaced and the cells incubated for a further hour. Images from HAp sponges were taken using an inverted microscope (Leica DMIRB/E), equipped with a fluorescence filter enabling fluorescent imaging.

Samples were fixed with 4% paraformaldehyde or 95% ethanol, depending on the staining protocol, prior to immunocytochemical and histochemical analysis. For alcian blue/sirius red staining, HAp sponges were fixed in 75% ethanol and further fixed in 100% formaldehyde for 45 min prior to embedding in paraffin wax. Thin sections (7 μm) were cut on a rotary microtome and sections were stained using Weigert haematoxylin solutions prior to staining with 0.5% alcian blue. After treatment with 1% molybdophosphoric acid, samples were stained using 0.1% sirius red.

Histological detection of alkaline phosphatase was performed following fixation in 95% (v/v) ethanol using a Sigma alkaline phosphatase kit (no. 85) according to the manufacturer's instructions in order to assess metabolic activity and viability of the cells. Alkaline phosphatase specific enzyme activity was measured using *p*-nitrophenyl phosphate as substrate in 2-amino-2-methyl-1-propanol alkaline buffer solution (1.5 M, pH 10.3 at 25 °C) and DNA content was measured using PicoGreen as per the manufacturer's instructions (Molecular Probes, Leiden, Netherlands). Specific activity was expressed as nanomoles of *p*-nitrophenol phosphate/h/μg DNA.

3. Results and discussion

3.1. Sponge formation and characterisation

Dispersions of HAp nanoparticles were prepared by methods previously described (experimental methods) [12]. Synthesis in the presence of alanine, arginine or aspartic acid produced aqueous suspensions of HAp nanoparticles that were needle- or rod-shaped with mean particle lengths of 60, 80 and 150 nm, respectively. Addition of dextran sulphate ($M_r \sim 500$k) to nanoparticle dispersions containing an excess of the amino acids gave an immediate yellow coloration. Corresponding UV–vis spectra showed a shoulder peak at 280 nm associated with interactions between the carbonyl auxochromic and amino chromophoric [18] end groups of dextran and amino acids, respectively.

Controlled heating of the air-dried yellow pastes up to a temperature of 800 °C produced intact sponge-like HAp monoliths with retention of the macroscopic

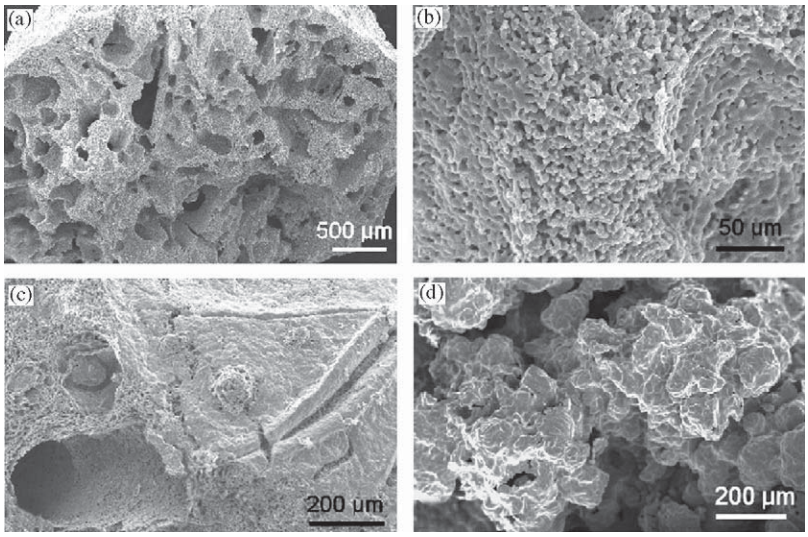

Fig. 1. SEM images of sponge-like monoliths prepared from dextran sulphate/HAp pastes in the presence of (a,b) aspartic acid, (c) alanine and (d) arginine.

morphology. The materials were designated as HAp/D, HAp/A or HAp/R, depending on whether aspartic acid (D), alanine (A) or arginine (R) was used in the mixture. In all cases, XRD measurements showed reflections at $d = 2.81$, 2.78 and 2.72 Å corresponding to the (2 1 1), (1 1 2) and (3 0 0) planes, respectively, of well-crystalline carbonated HAp. This was confirmed by FT-IR spectroscopy that showed absorbance bands for PO_4^{3-} ($\sim$565, 605 and 1028 cm^{-1}), OH ($v_s \sim 3650\,cm^{-1}$) and CO_3^{2-} ($v_3 \sim 1460\,cm^{-1}$).

SEM investigations indicated that the HAp/D, HAp/A and HAp/R monoliths exhibited different micro-architectures. The HAp/D replicas consisted of an interconnected network of relatively large pores ca. 200 μm across, with a roughened internal wall structure composed of closely packed sintered HAp particles (Fig. 1a,b). The observations were consistent with the in situ organization, aggregation and coalescence of pre-formed HAp nanoparticles within the boundary regions of a foam-like organic template produced by trapping of steam, CO_2 and O_2 gas bubbles during thermal degradation of the dextran sulphate matrix. In contrast, the HAp/A sponges consisted in general of smaller pores (100–150 μm) due to enhanced fusion of the HAp nanoparticles during thermal processing (Fig. 1c). The reduction in pore size was even more apparent for the HAp/R monoliths, which showed increased levels of compaction and discontinuity in the internal structure due to excessive agglomeration of the inorganic particles (Fig. 1d). Significantly, no sponge-like monoliths were produced on heating dextran sulphate-based composites prepared in the presence of dialysed dispersions of the HAp nanoparticles, indicating that excess amounts of amino acid were required to produce intact macro-porous materials.

Similar experiments using dextran sulphate were also undertaken at 800 °C, but with the sintering time reduced from 6 to 1 h using heating rates of either 10 or 1°/min. Decreasing the heating time produced sponges with less mechanical stability, although with relatively similar macroporosity, indicating that increased sintering times yielded stronger materials. Decreasing the heating rate also reduced the sponge macroporosity, suggesting that slow rates of dextran degradation did not produce stable foam-like expanded intermediates with sufficient stability to act as templates for inorganic replication.

Other studies indicated that changes in the charge associated with the dextran matrix had a significant effect on the micro-architecture of the HAp replicas. For example, thermal processing of pastes prepared from an unfunctionalised dextran with a similar molecular weight (500k) produced HAp materials of significantly different structure and morphology (Fig. 2). For example, no sponge-like materials were observed in the presence of aspartic acid; instead compacted aggregates of micrometre-sized HAp particles were produced (Fig. 2a). In contrast, delicate sponges consisting of filaments of coalesced HAp particles approximately 1–5 and 0.5 μm in length and width, respectively, were obtained from dextran/HAp pastes containing alanine (Fig. 2b). These materials were extremely fragile and did not readily retain their 3-D macroporosity during sample preparation procedures. Similar micro-structures were prepared with arginine, although the HAp filaments were somewhat shorter in length (< 1 μm) (Fig. 2c).

The above results clearly indicated that formation of the HAp sponge micro-architecture was dependent on the interplay of several factors, including heating rates

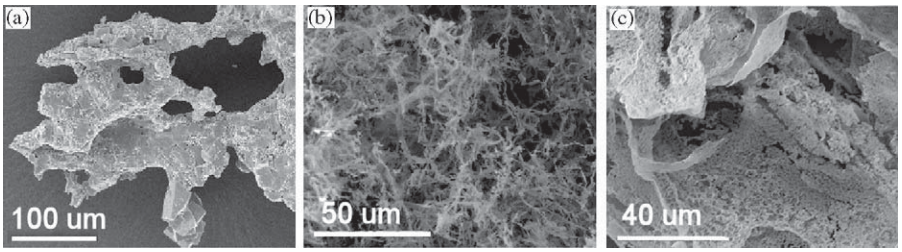

Fig. 2. SEM images of HAp materials prepared using unfunctionalised dextran in the presence of (a) aspartic acid, (b) alanine and (c) arginine.

and sintering times, type of amino acid used, and chemical nature of the dextran matrix. (Other factors, such as changes in the molecular weight of dextran, also had significant effects (data not included).) For dextran sulphate, strong electrostatic attraction between the amino acid additive and polysaccharide matrix, for example in the presence of arginine, significantly reduced the size and interconnectivity of the macropores; thus, the most promising materials were produced using negatively charged aspartic acid. However, replacing dextran sulphate with unfunctionalised dextran did not produce intact macroporous monoliths for any of the amino acids investigated, suggesting that some degree of electrostatic interaction, presumably involving the protonated α-amino group of the additive and sulphated side chain of the polysaccharide, was required for effective structuration. One possibility is that these relatively weak interactions help to stabilise the expanded foam-like template produced in situ during thermal processing, with the consequence that aggregation and subsequent sintering of the HAp nanoparticles take place with a high degree of spatial organisation.

3.2. Biocompatibility studies

Biocompatibility studies were undertaken by examining the viability, adhesion, spreading and proliferation of human bone marrow (HBM) stromal cells in the presence of HAp/D and HAp/A sponges over a period of 14 days. In both cases, cell viability was indicated by an intense green fluorescence due to incorporation of the Cell Tracker green CMFDA fluorescent probe into the cell cytoplasm. Negligible incorporation of Ethidium Homodimer-1 was observed, indicating that few necrotic cells were present over this time period. Significantly, histological detection of extensive alkaline phosphatase expression in samples of HAp/A and HAp/D sponges seeded with HBM stromal cells confirmed cell viability, metabolic activity and maintenance of the osteoblast phenotype in culture (Fig. 3a,c). In addition, the cells showed morphological evidence of new bone matrix formation, as visualised by alcian blue staining for proteoglycans and sirius red staining indicative of collagen deposition (Fig. 3b,d). Quantitative determination of alkaline phosphatase specific enzyme activities revealed that the rates (ca. 2.5×10^3 nmol *p*-nitrophenol phosphate/μg DNA/h) were similar for HBM stromal cells grown on the HAp/D sponges and control experiments using these cells but grown on tissue culture plastic. In contrast, HBM stromal cells grown in the presence of the HAp/A sponges showed a significant decrease in activity (ca. 1.5×10^3 nmol *p*-nitrophenol phosphate/μg DNA/h), presumably due to the reduced macroporosity of this material. However, extensive penetration of the HBM stromal cells into the surface pores and internal structure of the HAp sponges (osteoconductivity) was not observed, and disintegration and degradation of the structure was apparent after 3 weeks.

4. Conclusions

In conclusion, our results indicate that sponge-like calcium phosphate monoliths can be readily prepared by template-directed aggregation of preformed amino-acid-functionalised HAp nanoparticles within thermally degraded dextran sulfate pastes. Significantly, such materials could not be prepared in the absence of excess amino acids or the presence of non-anionic dextran, indicating that along with physical parameters such as heating rate and sintering time, chemical interactions between the matrix and additive were important in controlling the spatial organisation and aggregation of the HAp nanoparticles. In terms of potential biomaterials applications, materials prepared using dextran sulphate in the presence of aspartic acid appear to be most promising in terms of macroscopic shape persistence, large pore sizes (>100 μm) and excellent in vitro biocompatibility. However, these monoliths as currently fabricated would have limited potential for load-bearing applications such as bone implantation [19], but in contrast could be useful for cartilage or soft tissue engineering. Further work based on this novel fabrication method will focus on improving the mechanical strength of the sponges, increasing the pore interconnectivity for osteoconductivity, with the long-term aim

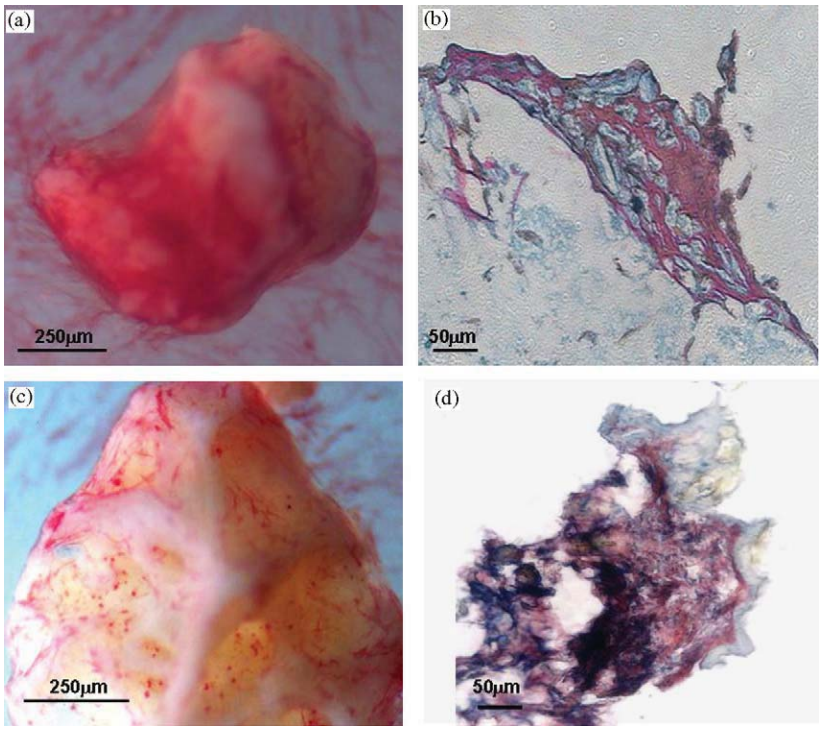

Fig. 3. Photomicrographs of HBM stromal cells grown for 14 days on HAp/A and HAp/D sponge-like scaffolds showing, respectively, (a,c) expression of alkaline phosphatase (red staining) and (b,d) collagen matrix production (sirius red/alcian blue staining).

of producing new scaffold-like template designs for application in tissue regeneration.

References

[1] Ramay HR, Zhang M. Preparation of porous hydroxyapatite scaffolds by combination of gel-casting and polymer sponge methods. Biomaterials 2003;24:3293–302.

[2] Padilla S, Roman J, Vallet-Regi M. Synthesis of porous hydroxyapatites by combination of gelcasting and foams burn out methods. J Mater Sci: Mater Med 2002;13:1193–7.

[3] Tadic D, Beckmann F, Schwarz K, Epple M. A novel method to produce hydroxyapatite objects with interconnecting porosity that avoids sintering. Biomaterials 2004;25:3335–40.

[4] Zhang Y, Zhang MQ. Three-dimensional macroporous calcium phosphate bioceramics with nested chitosan sponges for load-bearing bone implants. J Biomed Mater Res 2002;61(1):1–8.

[5] Tachibana A, Kaneko S, Tanabe T, Yamaguchi K. Rapid fabrication of keratin-hydroxyapatite hybrid sponges toward osteoblast cultivation and differentiation. Biomaterials 2005;26:297–302.

[6] Ma J, Wang C, Peng KW. Electrophoretic deposition of porous hydroxyapatite scaffold. Biomaterials 2003;24:3505–10.

[7] Wilson CE, de Bruijn JD, van Blitterswijk CA, Verbout AJ, Dhert WJA. Design and fabrication of standardized hydroxyapatite scaffolds with a defined macro-architecture by rapid prototyping for bone-tissue-engineering research. J Biomed Mater Res A 2004;68A(1):123–32.

[8] Muzzarelli R, Biagini G, Pugnaloni A, Filippini O, Baldassarre V, Castaldini C, Rizzoli C. Reconstruction of parodontal tissue with chitosan. Biomaterials 1989;10:598–603.

[9] de Groot K. Bioceramics consisting of calcium phosphate salts. Biomaterials 1980;1(47):47–50.

[10] Chang BS, Lee CK, Hong KS, Youn HJ, Ryu HS, Chung SS, Park KW. Osteoconduction at porous hydroxyapatite with various pore configurations. Biomaterials 2000;21:1291–8.

[11] Yuan H, Yang Z, de Bruijn JD, de Groot K, Zhang X. Material-dependent bone induction by calcium phosphate ceramics: a 2.5-year study in dog. Biomaterials 2001;22:2617–23.

[12] Gonzalez-McQuire R, Chane-Ching JY, Vignaud E, Lebugle A, Mann S. Synthesis and characterization of amino acid-functionalized hydroxyapatite nanorods. J Mater Chem 2004;14:2277–81.

[13] Walsh D, Aracelli L, Ikoma T, Tanaka J, Mann S. Dextran templating for the synthesis of metallic and metal oxide sponges. Nat Mater 2003;2(6):386–90.

[14] Li Y, Spencer HG. Adsorption of dextrans on spherical TiO_2 particles. Coll Surf 1992;66:189–95.

[15] Spaltro S, Ananthapasmanabhan KP, Frushour M, Aronson M. Adsorption of dextrans onto hydroxyapatite: presence of maxima. Coll Surf 1992;68(1):8.

[16] Hlady V. Adsorption of dextran and dextran sulfate on precipitated calcium oxalate monohydrate. J Coll Interface Sci 1984;98:373–84.

[17] Hardikar VV, Matijevic E. Influence of ionic and nonionic dextrans on the formation of calcium hydroxide and calcium carbonate particles. Colls Surf A: Physchem Eng Asp 2001;186:23.

[18] Christie RM. Colour Chemistry. Cambridge: Royal Society of Chemistry; 2001.

[19] Lutton C, Read J, Trau M. Nanostructured biomaterials: a novel approach to artificial bone implants. Aust J Chem 2001; 54:621–3.